JCI The Journal of Clinical Investigation

Amendment history:
- Erratum (July 2003)

The voltage-gated Kv1.3 K^+ channel in effector memory T cells as new target for MS

Heike Wulff, … , Christine Beeton, K. George Chandy

J Clin Invest. 2003;111(11):1703-1713. https://doi.org/10.1172/JCI16921.

Article **Autoimmunity**

Through a combination of fluorescence microscopy and patch-clamp analysis we have identified a striking alteration in K^+ channel expression in terminally differentiated human $CCR7^-CD45RA^-$ effector memory T lymphocytes (T_{EM}). Following activation, T_{EM} cells expressed significantly higher levels of the voltage-gated K^+ channel Kv1.3 and lower levels of the calcium-activated K^+ channel IKCa1 than naive and central memory T cells (T_{CM}). Upon repeated in vitro antigenic stimulation, naive cells differentiated into $Kv1.3^{high}IKCa1^{low}$ T_{EM} cells, and the potent Kv1.3-blocking sea anemone *Stichodactyla helianthus* peptide (ShK) suppressed proliferation of T_{EM} cells without affecting naive or T_{CM} lymphocytes. Thus, the $Kv1.3^{high}IKCa1^{low}$ phenotype is a functional marker of activated T_{EM} lymphocytes. Activated myelin-reactive T cells from patients with MS exhibited the $Kv1.3^{high}IKCa1^{low}$ T_{EM} phenotype, suggesting that they have undergone repeated stimulation during the course of disease; these cells may contribute to disease pathogenesis due to their ability to home to inflamed tissues and exhibit immediate effector function. The $Kv1.3^{high}IKCa1^{low}$ phenotype was not seen in glutamic acid decarboxylase, insulin-peptide or ovalbumin-specific and mitogen-activated T cells from MS patients, or in myelin-specific T cells from healthy controls. Selective targeting of Kv1.3 in T_{EM} cells may therefore hold […]

The voltage-gated Kv1.3 K^+ channel in effector memory T cells as new target for MS

Heike Wulff,[1] Peter A. Calabresi,[2] Rameeza Allie,[2] Sung Yun,[2] Michael Pennington,[3] Christine Beeton,[1] and K. George Chandy[1]

[1]Department of Physiology and Biophysics, University of California Irvine, College of Medicine, Irvine, California, USA
[2]Department of Neurology, University of Maryland School of Medicine, Baltimore, Maryland, USA
[3]Bachem Bioscience Inc., King of Prussia, Pennsylvania, USA

Through a combination of fluorescence microscopy and patch-clamp analysis we have identified a striking alteration in K^+ channel expression in terminally differentiated human $CCR7^-CD45RA^-$ effector memory T lymphocytes (T_{EM}). Following activation, T_{EM} cells expressed significantly higher levels of the voltage-gated K^+ channel Kv1.3 and lower levels of the calcium-activated K^+ channel IKCa1 than naive and central memory T cells (T_{CM}). Upon repeated in vitro antigenic stimulation, naive cells differentiated into $Kv1.3^{high}IKCa1^{low}$ T_{EM} cells, and the potent Kv1.3-blocking sea anemone *Stichodactyla helianthus* peptide (ShK) suppressed proliferation of T_{EM} cells without affecting naive or T_{CM} lymphocytes. Thus, the $Kv1.3^{high}IKCa1^{low}$ phenotype is a functional marker of activated T_{EM} lymphocytes. Activated myelin-reactive T cells from patients with MS exhibited the $Kv1.3^{high}IKCa1^{low}$ T_{EM} phenotype, suggesting that they have undergone repeated stimulation during the course of disease; these cells may contribute to disease pathogenesis due to their ability to home to inflamed tissues and exhibit immediate effector function. The $Kv1.3^{high}IKCa1^{low}$ phenotype was not seen in glutamic acid decarboxylase, insulin-peptide or ovalbumin-specific and mitogen-activated T cells from MS patients, or in myelin-specific T cells from healthy controls. Selective targeting of Kv1.3 in T_{EM} cells may therefore hold therapeutic promise for MS and other T cell–mediated autoimmune diseases.

J. Clin. Invest. **111**:1703–1713 (2003). doi:10.1172/JCI200316921.

Introduction

Autoreactive memory T lymphocytes have been implicated in the pathogenesis of MS (1–4), type 1 diabetes mellitus (5), and psoriasis (6). In MS (7–9), myelin-reactive lymphocytes exhibit a memory phenotype (1–4) and are believed to contribute to the inflammatory attack on the central nervous system because of their ability to induce experimental autoimmune encephalomyelitis (EAE) in animals (10, 11), a model for MS. Strategies designed to specifically suppress the function of chronically activated memory T cells without impairing the function of naive T cells might therefore have value in the treatment of autoimmune diseases.

The voltage-gated K^+ channel (Kv1.3) and the calcium-activated K^+ channel (IKCa1) regulate membrane potential and Ca^{2+} signaling in T lymphocytes (12–16). Due to the restricted tissue distribution of these channels and the availability of specific and potent inhibitors, Kv1.3 and IKCa1 are widely recognized as potential therapeutic targets for immunotherapy (16, 17). We recently reported a novel K^+ channel pattern in chronically activated encephalitogenic myelin-reactive rat memory T cells (18, 19). These cells upregulated Kv1.3 expression after activation with myelin antigens with no change in IKCa1 levels, in contrast to naive rat and human T cells that upregulate IKCa1 with little change in Kv1.3 expression following activation (12–16, 20–22). Adoptive transfer of myelin-specific $Kv1.3^{high}IKCa1^{low}$ memory cells into rats produced severe EAE, and selective inhibition of the Kv1.3 channel effectively prevented and treated disease (18, 23). In the present study, we used the patch-clamp technique in combination with fluorescence microscopy and flow cytometry to determine whether the distinctive $Kv1.3^{high}IKCa1^{low}$ channel pattern is found in human memory cells, and in particular in myelin-reactive T cells from MS patients.

In humans, two subsets of memory T lymphocytes, central memory T cells (T_{CM}) and effector memory T cells (T_{EM}), have been described based on the expression

Received for publication September 16, 2002, and accepted in revised form February 27, 2003.

Address correspondence to: K. George Chandy, Department of Physiology and Biophysics, Room 291 Joan Irvine Smith Hall, College of Medicine, University of California Irvine, Health Sciences Center Drive, Irvine, California 92697, USA.
Phone: (949) 824-2133; Fax: (949) 824-3143;
E-mail: gchandy@uci.edu.
Heike Wulff and Peter A. Calabresi contributed equally to this work.

Conflict of interest: The authors have declared that no conflict of interest exists.

Nonstandard abbreviations used: experimental autoimmune encephalomyelitis (EAE); voltage-gated K^+ channel (Kv1.3); calcium-activated K^+ channel (IKCa1); effector memory T cells (T_{EM}); central memory T cells (T_{CM}); T cell line (TCL); myelin basic protein (MBP); proteolipid protein (PLP); myelin oligodendrocyte glycoprotein (MOG); tetanus toxoid (TT); glutamic acid decarboxylase 65 (GAD65); thymidine (TdR); phycoerythrin (PE); *Stichodactyla helianthus* peptide (ShK); ShK with diaminopropionic acid at position 22 (Dap^{22}).

of the chemokine receptor CCR7 and the phosphatase CD45RA (24, 25). Naive ($CCR7^+CD45RA^+$) and T_{CM} ($CCR7^+CD45RA^-$) cells require antigen priming in lymph nodes before they migrate to inflammatory sites, whereas terminally differentiated T_{EM} cells ($CCR7^-CD45RA^-$) rapidly enter inflamed tissues, produce copious amounts of IFN-γ and IL-4, and exhibit immediate effector function. Here we demonstrate that the $Kv1.3^{high}IKCa1^{low}$ channel phenotype is found exclusively in activated human T_{EM} cells, whereas naive and T_{CM} cells remain $Kv1.3^{low}$ and upregulate IKCa1 upon activation. Myelin-reactive T cells from MS patients are predominantly T_{EM} cells and exhibit the $Kv1.3^{high}IKCa1^{low}$ channel pattern after activation with myelin antigens, suggesting that they have undergone multiple rounds of antigenic stimulation during the course of disease. A high-affinity Kv1.3 inhibitor specifically suppressed proliferation of T_{EM} cells at picomolar concentrations without persistently affecting the function of naive or T_{CM} lymphocytes. Selective inhibition of Kv1.3 channels in T_{EM} cells may therefore be a potential approach for therapy of MS and other T cell–mediated autoimmune disorders.

Table 1
Clinical data for the MS patients studied

Patient	Age	Sex	MS Type	MS Duration	EDSS
1	53	Male	PPMS	5 years	3.5
2	47	Female	RRMS	5 months	2.0
3	50	Female	SPMS	20 years	4.0
4	32	Female	RRMS	3 months	0
5	48	Female	RRMS	10 months	2.0
6	43	Female	RRMS	2 years	0
7	41	Female	RRMS	3 months	1.5
8	41	Female	RRMS	3 years	1.5
9	51	Female	RRMS	2 years	3.0
10	45	Female	RRMS	17 years	1.5
11	55	Female	RRMS	25 years	1.0
12	55	Female	RRMS	3 years	3.0
13	49	Female	RRMS	7 years	2.0
14	40	Male	RRMS	2 years	1.5
15	34	Female	RRMS	6 months	2.5
16	63	Female	SPMS	30 years	6.0
17	45	Female	RRMS	10 years	1.5
18	29	Female	RRMS	6 years	1.5
19	37	Female	RRMS	3 years	1.5
20	39	Female	RRMS	2 years	2.0

EDSS, Kurtzke's expanded disability status score, a ten-level clinical scale; PPMS, primary progressive MS; RRMS, relapsing remitting MS; SPMS, secondary progressive MS. Duration is the length of disease from time of diagnosis to the beginning of the study.

Methods

Patients. T cells from 20 MS patients (defined according to McDonald criteria) and six healthy volunteers were used in this study. None of the patients had received immunotherapy and none was receiving primary treatment at the time blood was drawn. The clinical features of the patients are shown in Table 1.

Generation of T cell lines. T cell lines (TCLs) specific for myelin basic protein (MBP; 10 μg/ml), proteolipid protein (PLP) peptide 139-151 (5 μg/ml), myelin oligodendrocyte glycoprotein (MOG) peptide 35-55 (5 μg/ml), tetanus toxoid (TT; 10 μg/ml), glutamic acid decarboxylase 65 (GAD65) peptide 555-567 (5 μg/ml), insulin B peptide 9-23 (5 μg/ml), and chicken ovalbumin peptide 323-339 (5 μg/ml) were generated according to a previously described split-well assay (26). MBP was obtained from Sigma-Aldrich (St. Louis, Missouri, USA), PLP and MOG from Mixture Sciences Inc. (San Diego, California, USA), TT from the University of Massachusetts Toxicology Laboratory (Cambridge, Massachusetts, USA), and GAD65, insulin peptide, and ovalbumin from Bachem Bioscience Inc. (King of Prussia, Pennsylvania, USA). Briefly, whole blood samples, or in some cases leukapheresis samples (All Cells Inc., San Francisco, California, USA), were collected from consenting healthy subjects or patients with MS according to a protocol approved by the University of Maryland Institutional Review Board. PBMCs, isolated by density gradient centrifugation as described (27), were cultured in Iscove's modified Dulbecco's medium supplemented with 2 mM glutamine, 100 U/ml penicillin, 100 μg/ml streptomycin, 50 μg/ml gentamicin (BioWhittaker Inc., East Rutherford, New Jersey, USA) and 5% human serum (Sigma-Aldrich). Cells were seeded at 2×10^5 cells/well (200 μl/well) in round-bottom 96-well plates (Corning-Costar Corp., Cambridge, Massachusetts, USA) and cultured at 37°C in the presence of antigen. IL-2 (20 U/ml, courtesy of NIH, Biological Resources Branch) was added on day 7. At day 14, one-half of the contents of each well was used to set up daughter plates to test for antigen-specific proliferation. Duplicate wells were cultured with or without antigen and fresh medium containing 1×10^5 irradiated autologous PBMCs. Cells were cultured for 3 days, and 1 μCi of [^{3}H]thymidine ([^{3}H]TdR) (Amersham Pharmacia Biotech, Piscataway, New Jersey, USA) was added to each well for the last 16 hours of culture. Cells were harvested onto filters and incorporation of [^{3}H]TdR was quantified on a Betaplate (PerkinElmer Life Sciences, Boston, Massachusetts, USA). Parallel parent plates were also restimulated in the same manner. TCLs from parent wells with a stimulation index greater than two on day 7 after restimulation (21 total days in culture), as identified in matched daughter plates, were studied by FACS analysis. Short-term TCLs were stimulated three times with antigen at regular 7-day cycles, while longer-term TCLs were stimulated seven, ten, or twelve times. Short-term TCLs were 80–90% $CD4^+$ and long-term TCLs were 100% $CD4^+$. The average stimulation index was 4.9 ± 0.9 (SD) for the myelin antigen–reactive TCLs and 3.7 ± 0.2 for the TT-reactive TCLs. Previous studies using the split-well assay have demonstrated that with antigens that have a low precursor frequency, such as MBP, the likelihood of having clones in a single well is high (28).

Isolation of $CD4^+$ or $CD8^+$ T cells from peripheral blood. $CD4^+$ and $CD8^+$ T cells were isolated from peripheral

blood of controls with RosetteSep (StemCell Technologies Inc., Vancouver, British Columbia, Canada). Purity was determined by staining with phycoerythrin-conjugated (PE-conjugated) mAb's ($CD4^+$ from Molecular Probes Inc., Eugene Oregon, USA; $CD8^+$ from Pharmingen, San Diego, California, USA) and was found to be greater than 95% for both the $CD4^+$ and $CD8^+$ populations by FACS analysis.

FACS analysis. $CD4^+$ TCLs were stained with combinations of fluorochrome-conjugated isotype controls or fluorochrome-conjugated mAb's to CD4 and CD45RA along with unconjugated anti–human CCR7 mAb (2H4) followed by a secondary biotinylated rat anti–mouse IgM mAb and then by streptavidin-PE (Pharmingen). $CD8^+$ peripheral blood T cells were stained with FITC-conjugated anti–human CCR7 mAb (clone 150503; R&D Systems Inc., Minneapolis, Minnesota, USA) and PE-conjugated anti–human CD45RA mAb (HI100; Pharmingen). Stained cells were analyzed by flow cytometry on a FACSVantage with CellQuest software (Becton, Dickinson and Co., Franklin Lakes, New Jersey, USA).

Electrophysiology. T cells were patch clamped in the whole-cell configuration before or 48 hours after stimulation with antigen, anti-CD3 mAb, or PMA plus ionomycin (12, 15). Kv1.3 currents were elicited by repeated 200-ms pulses from a holding potential of –80 mV to 40 mV, applied every second to visualize Kv1.3's characteristic cumulative inactivation, or every 30 seconds in experiments to measure blocking by *Stichodactyla helianthus* peptide (ShK) or ShK with diaminopropionic acid at position 22 (ShK-Dap^{22}). Kv1.3 currents were recorded in normal Ringer solution with a Ca^{2+}-free pipette solution containing (in mM): 145 KF, 10 HEPES, 10 EGTA, and 2 $MgCl_2$, pH 7.2, 300 mOsm. Whole-cell Kv1.3 conductances were calculated from the peak current amplitudes at 40 mV.

IKCa1 currents were elicited with voltage ramps from –120 to 40 mV of 200 ms duration applied every 10 seconds in the presence of 1 nM of ShK-Dap^{22} to block Kv1.3 currents. The pipette solution contained (in mM): 145 K^+ aspartate, 2 $MgCl_2$, 10 HEPES, 10 K_2EGTA, and 8.5 $CaCl_2$ (1 μM free Ca^{2+}), pH 7.2, 290 mOsm. To reduce chloride "leak" currents, we used a Na^+ aspartate external solution containing (in mM): 160 Na^+ aspartate, 4.5 KCl, 2 $CaCl_2$, 1 $MgCl_2$, and 5 HEPES, pH 7.4, 300 mOsm. Whole-cell IKCa1 conductances were calculated from the slope of the current-voltage relationship at –80 mV.

Kv1.3 and IKCa1 channel numbers per cell were determined by dividing the whole-cell Kv1.3 or IKCa1 conductance by the single-channel conductance value for each channel (Kv1.3, 12 pS; IKCa1, 11 pS) (15, 29). Cell capacitance, a direct measure of cell surface area, was constantly monitored during recording. Resting (unstimulated) T cells had membrane capacitances below 2 pF (cell diameter less than 7 μm), while activated cells had membrane capacitances greater than 4 pF (cell diameter greater than 11 μm). To normalize for cell size, we determined Kv1.3 and IKCa1 channel densities per μm^2 cell surface area by dividing the average channel number/cell by the average cell surface area determined from capacitance measurements (1 pF = 100 μm^2).

$CD4^+$ short-term and long-term TCLs specific for MBP, PLP, MOG, or TT, from MS patients or healthy volunteers (control subjects), were patch clamped before or 48 hours after stimulation with antigen. $CD4^+$ or $CD8^+$ peripheral blood T cells from healthy volunteers or MS patients were also analyzed before or 48 hours after stimulation with either 50 ng/ml anti-CD3 mAb (Biomeda Corp., Hayward, California, USA) in the presence of autologous irradiated PBMCs (25 Gy) or with a combination of 10 nM PMA and 175 nM ionomycin. In all experiments T cells were distinguished from irradiated APCs by their staining, size, and undamaged appearance. Statistical differences in channel number/cell or channel density were determined by Student *t* test.

Immunostaining and electrophysiology. Channel expression was studied in single $CD4^+$ naive ($CCR7^+CD45RA^+$), T_{CM} ($CCR7^+CD45RA^-$), or T_{EM} ($CCR7^-CD45RA^-$) cells. Cells were stained for CCR7 and CD45RA on ice in RPMI medium (supplemented with 10% FCS) with mouse anti–human CCR7 mAb (2H4, Pharmingen) followed by FITC-conjugated rat anti–mouse IgM mAb (R6-60.2, Pharmingen). After blocking with 20% mouse serum, cells were stained with PE-conjugated anti–human CD45RA mAb (HI100, Pharmingen). Cells were washed, put on poly-L-lysine–coated coverslips, and kept in the dark at 4°C for 10–30 minutes to attach. Naive, T_{CM}, and T_{EM} cells were visualized by fluorescence microscopy and patch clamped immediately. Naive cells were identified in a $CD4^+$ T cell population isolated from controls. T_{CM} and T_{EM} cells were identified in $CD4^+$ MBP- or TT-specific TCLs. In other experiments, $CD4^+$ or $CD8^+$ T cells isolated from the peripheral blood of controls were stained with FITC-conjugated anti–human CCR7 mAb (clone 150503; R&D Systems Inc.) and PE-conjugated anti–human CD45RA mAb. $CD4^+$ or $CD8^+$ naive, T_{CM}, and T_{EM} cells were then visualized by fluorescence microscopy and patch clamped.

Proliferation assay. MBP-specific TCLs and freshly isolated PBMCs were triggered with the identical stimulus (50 ng/ml soluble anti-CD3 mAb). A $CD4^+$ MS patient TCL stimulated three times with MBP, and a $CD4^+$ control TCL stimulated 12 times with MBP were rested for 10 days in 20 U/ml IL-2 after the last antigenic stimulation prior to being reactivated for the proliferation assay. Both of these TCLs comprised primarily T_{EM} cells, as determined by FACS analysis. TCL cells (5×10^4) were incubated for 72 hours with 5×10^4 autologous irradiated PBMCs in complete RPMI medium in 96-well plates, in the presence or absence of anti-CD3 mAb and with or without ShK (Bachem Bioscience Inc.). [^{3}H]TdR (1 μCi/well) was added for the last 16 hours of culture and [^{3}H]TdR incorporation was determined. Background counts in unstimulated (resting) TCLs were below 500 cpm, and maximal counts in anti-CD3 mAb–activated cells (in the absence of ShK) were

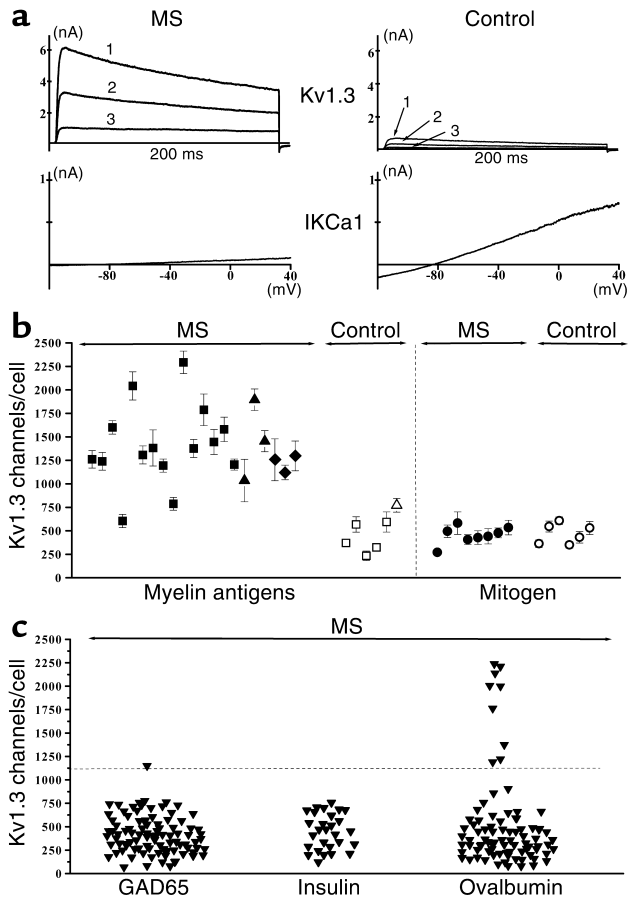

Figure 1

Myelin antigen–activated T cells from MS patients express the distinctive Kv1.3^{high}IKCa1^{low} phenotype. (**a**) Kv1.3 and IKCa1 currents in TCLs from MS patients and controls measured 48 hours after activation with MBP. The numbers 1, 2, and 3 in the Kv1.3 traces represent traces after the first, second, and third depolarizing 200-ms pulse; the pulse interval is 1 second. (**b**) Kv1.3 channel number/cell in myelin antigen–activated TCLs (left) or mitogen-activated T cells (right) from MS patients or controls. Each data point constitutes the mean ± SEM of 20–30 cells from two to seven independent TCLs. Myelin antigens used were MBP (filled and open squares), MOG (filled and open triangles), and PLP (filled diamonds). Filled symbols, MS patients; open symbols, control subjects. Mitogens used were soluble anti-CD3 mAb (50 ng/ml) and PMA (10 nM) plus ionomycin (175 nM) (data for both mitogens are grouped together). Filled circles, MS patients; open circles, controls. (**c**) Kv1.3 channel number/cell in MS patient T cells activated for 48 hours with the control antigens GAD65, insulin peptide, and ovalbumin. Due to the paucity of cells in these TCLs, IKCa1 expression was measured in only two to three cells per TCL.

20,000–30,000 cpm. The counts in the presence of ShK (the blocker) were normalized to the maximal counts from the same experiment using this formula: (blocker cpm – resting cpm)/(maximal cpm – resting cpm).

PBMCs from three healthy volunteers (1×10^5 cells per well) were stimulated with anti-CD3 mAb for 48 hours with or without ShK. One aliquot was pulsed with [^{3}H]TdR for the last 12 hours and [^{3}H]TdR incorporation was measured. The counts in the presence of ShK were determined as above (resting counts below 500 cpm, maximal counts about 30,000 cpm). The second aliquot was washed thoroughly and then rested in medium for 16 hours. Then it was rechallenged for 48 hours with anti-CD3 mAb with or without ShK. During the last 12 hours it was pulsed with [^{3}H]TdR, and then [^{3}H]TdR incorporation was determined. Background counts were below 2,000 cpm for cells that were not reactivated with anti-CD3 mAb, and maximal counts in anti-CD3 mAb–reactivated cells were about 30,000 cpm. Blocker data were normalized as described above.

Results

Activated myelin-specific MS patient T cells exhibit a Kv1.3^{high}-IKCa1^{low} channel phenotype not found in activated myelin-specific control T cells. Figure 1a shows Kv1.3 and IKCa1 currents in short-term CD4$^+$ myelin antigen–specific TCLs from an MS patient and a healthy volunteer 48 hours after the third stimulation with MBP. The amplitude of the Kv1.3 current in the patient cell is strikingly greater than in the control cell, while the amplitude of the IKCa1 current is significantly smaller. This reciprocal difference could be due to an alteration in functional expression levels or to a simultaneous change in the properties of both channels. We found that Kv1.3 and IKCa1 channels in patient and control T cells had identical biophysical and pharmacological properties, indicating that the difference in Kv1.3 and IKCa1 current amplitudes is due to a change in functional expression. Kv1.3 currents exhibited "cumulative inactivation," a decrease in current amplitude during repetitive depolarizing pulses applied every second, which is characteristic of this channel (18, 29). They were also blocked by the peptide inhibitor ShK and its Kv1.3-specific analogue ShK-Dap^{22} with the same potency (ShK K_d, 9 ± 1 pM; ShK-Dap^{22} K_d, 64 ± 7 pM) as the cloned Kv1.3 channel (15, 30). The voltage-dependence, activation and inactivation kinetics, and all other channel parameters were consistent with these currents being solely Kv1.3 (data not shown) (12, 13, 15, 16, 18, 29). IKCa1 currents were fully activated by the presence of 1 μM cytoplasmic free Ca^{2+}, and the amplitude did not increase further at Ca^{2+} concentrations of 10 μM and 100 μM (not shown). IKCa1 currents also exhibited slight rectification, and were blocked by the selective IKCa1 inhibitor TRAM-34 with the same potency (K_d, 20 ± 5 nM) as the cloned channel (31).

We measured Kv1.3 channel number/cell in short-term myelin-specific CD4$^+$ TCLs from 20 MS patients (Table 1) and six healthy volunteers 48 hours after the third antigenic stimulation (Figure 1b). The majority of TCLs were MBP-specific, although cells from three patients and one control were specific for PLP or MOG. To ensure that only activated cells were studied, we patch clamped cells with membrane capacitances (a measure of the cell's surface area) greater than 4 pF, corresponding to a cell diameter greater than 11 μm, and excluded resting cells with membrane capacitances below 2 pF (diameter less than 7 μm). Corresponding to the increase in Kv1.3 current amplitude, Figure 1b demon-

strates that myelin antigen–activated patient T cells expressed significantly higher numbers of Kv1.3 channels/cell (1,489 ± 101 Kv1.3 channels/cell; mean ± SEM, n = 516 cells) than did myelin antigen–activated T cells from healthy controls (568 ± 82; n = 120 cells; P = 0.00004 by Student t test). When normalized for cell size, patient T cells had a threefold higher Kv1.3 channel density than did control cells (2.9 vs. 0.9 Kv1.3 channels/μm^2 surface area). In contrast, IKCa1 levels in patient cells (52 ± 4 IKCa1 channels/cell, 0.1 channels/μm^2, n = 56 cells) were fourfold lower than in control cells (186 ± 22 IKCa1 channels/cell, 0.4 channels/μm^2, n = 31 cells, P < 0.00001).

The Kv1.3^{high}IKCa1^{low} phenotype of myelin-specific MS patient T cells resembles the pattern seen in chronically activated myelin-specific encephalitogenic rat memory T cells (18, 19). Earlier studies have reported that quiescent human T cells express 200–400 Kv1.3 and about 10 IKCa1 channels per cell, and following activation upregulate IKCa1 via an AP1-dependent transcriptional mechanism with only a minimal increase in Kv1.3 expression. As expected, myelin-specific control T cells in the present study augmented IKCa1 expression (186 channels/cell) while not significantly increasing Kv1.3 (568 channels/cell) upon activation with myelin antigens. MS patient cells behaved differently, enhancing Kv1.3 levels (1,489 channels/cell) without a substantial increase in IKCa1 levels (52 channels/cell) following myelin-antigen stimulation, suggestive of a changed activation program.

To determine whether augmentation of functional Kv1.3 expression during activation is a general feature of all MS patient cells, we measured Kv1.3 channel numbers following mitogen activation in T cells from eight MS patients who had not begun immunotherapy and returned for clinical visits during the course of the study, and from six healthy controls. T cells were polyclonally activated for 48 hours through the T cell receptor with anti-CD3 mAb or with a combination of the PKC activator PMA and the Ca^{2+} ionophore ionomycin (the data for both sets of mitogens are grouped together because they were not different). The right panel of Figure 1b shows that the Kv1.3 channel number/cell in these mitogen-activated patient cells (465 ± 35 Kv1.3 channels/cell, n = 104 cells) was comparable to that in mitogen-activated control T cells (472 ± 40 Kv1.3 channels/cell, n = 95 cells), indicating that patient T cells, like control cells, do not upregulate Kv1.3 following mitogen activation.

As a further test, we measured Kv1.3 channel numbers in T cells from five MS patients specific for three control antigens. GAD65 and insulin peptide are autoantigens implicated in type 1 diabetes mellitus (5, 32, 33) but not MS, and ovalbumin is a common food antigen. Short-term TCLs specific for each of these antigens were generated in exactly the same way as myelin-specific TCLs and cells were patch clamped 48 hours after the third antigenic stimulation. Each data point in Figure 1c represents the Kv1.3 channel number in a single patient T cell; data from all five patients are grouped. The horizontal line in this figure indicates the lower limit (~1,100 Kv1.3 channels/cell, which represents the mean of 1489 minus three times the SEM value of 101) of Kv1.3 expression in myelin antigen–activated patient T cells. The majority of these patient cells did not enhance Kv1.3 upon activation, with the exception of one GAD65-specific cell (1/94 cells) and nine ovalbumin-specific (9/85) cells. The average Kv1.3 channel number/cell in myelin antigen–activated patient cells (1,489 ± 101 channels/cell) was significantly higher than in patient cells specific for GAD65 (420 ± 21, n = 94 cells, P < 0.00001), insulin peptide (479 ± 41, n = 29 cells, P = 0.00004), or

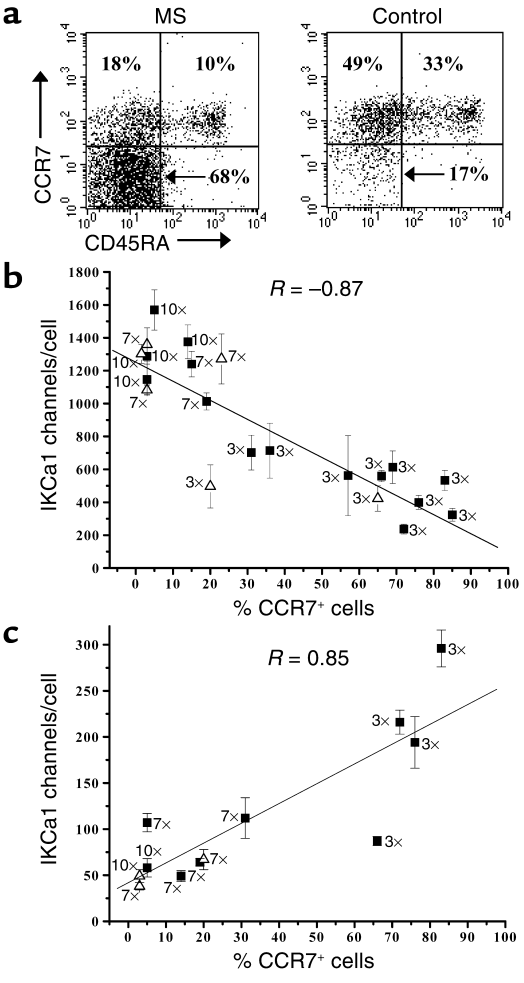

Figure 2
Cells with altered channel expression are phenotypically effector memory T cells. (**a**) Flow cytometry profiles showing CD45RA and CCR7 expression in MBP-specific TCLs from an MS patient and a control subject. (**b**) Kv1.3 channel number/cell versus percentage of CCR7$^+$ cells in control TCLs stimulated three, seven, and ten times with MBP (filled squares) or TT (open triangles). The number of antigenic stimulations is shown in the figure next to each symbol. Twenty or more cells were studied from each sample. (**c**) IKCa1 channel number/cell versus percentage of CCR7$^+$ cells in the same TCLs as in **b**. Fewer data points are included in the IKCa1 plot because the number of cells in some myelin antigen-specific TCL samples were not adequate to measure both Kv1.3 and IKCa1 expression in 20 cells each.

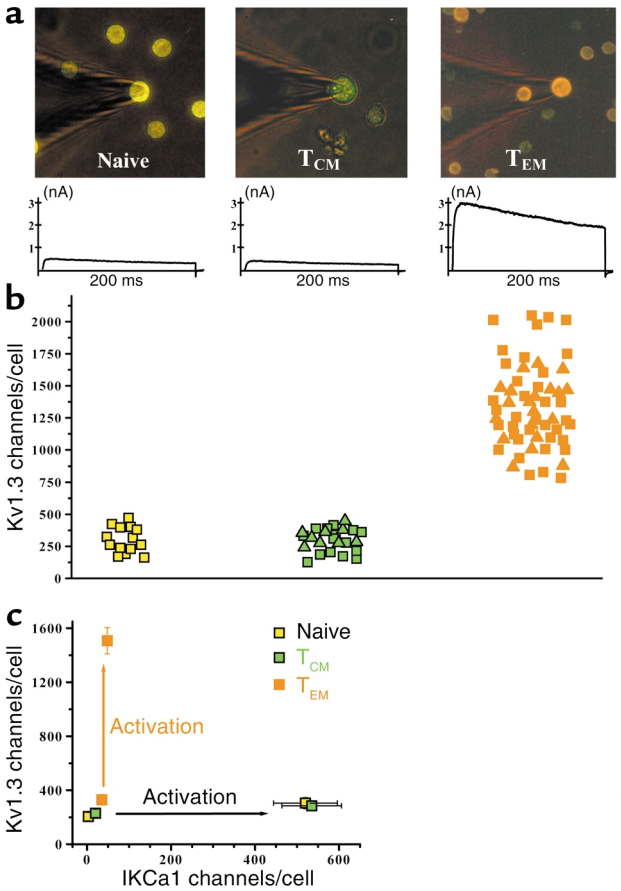

Figure 3

Kv1.3^{high}IKCa1^{low} phenotype: an exclusive functional marker for activated effector memory T cells. (**a**) Fluorescent immunostained images of patch-clamped CD4 T cell subsets from control subjects showing naive CCR7$^+$CD45RA$^+$ (left), T_{CM} CCR7$^+$CD45RA$^-$ cells (middle), and T_{EM} CCR7$^+$CD45RA$^+$ cells (right, counterstained with antihuman CD4 mAb). Representative Kv1.3 currents from each cell type are shown below the respective images. (**b**) Kv1.3 channel number/cell in naive (yellow squares), T_{CM} (MBP-stimulated, green squares; TT-stimulated, green triangles) and T_{EM} (MBP-stimulated, orange squares; TT-stimulated, orange triangles) T cells. Activated naive CD4$^+$ cells were identified in the peripheral blood of controls 48 hours following stimulation with anti-CD3 mAb. Activated T_{CM} and T_{EM} cells were identified in the same preparations of control TCLs (stimulated ten times with either MBP or TT) 48 hours after stimulation with the appropriate antigen. (**c**) Kv1.3 versus IKCa1 channel number per cell in the three populations before and after activation. Each data point is the mean ± SEM channel number in 20–50 cells.

ovalbumin (518 ± 54, n = 85, P = 0.00008). Collectively, the data in Figure 1 indicate that the myelin-specific T cell pool in MS patients differs from patient cells with other antigen specificities and from control cells in augmenting Kv1.3 expression instead of IKCa1 following activation.

Kv1.3^{high}IKCa1^{low} patient cells are activated T_{EM} cells. Since myelin-specific patient cells are reported to exhibit features of chronically stimulated memory T cells (1–4) and the Kv1.3^{high} IKCa1^{low} pattern is found in chronically activated rat memory T cells (18, 19), we suspected that the myelin antigen–activated patient cells with enhanced Kv1.3 expression might belong to a memory subset. In the FACS examples shown in Figure 2a, three distinct populations are seen in both patient and control TCLs based on expression of the chemokine receptor CCR7 and the phosphatase CD45RA; these correspond to naive (CCR7$^+$CD45RA$^+$), T_{CM} (CCR7$^+$CD45RA$^-$), and T_{EM} (CCR7$^-$CD45RA$^-$) lymphocytes (24, 25). The majority of lymphocytes in the patient's TCL expressed surface markers of the T_{EM} subset, whereas cells in the control's TCL exhibited markers of naive and T_{CM} subsets (Figure 2a). These FACS results along with the electrophysiology data in Figure 1 strongly suggest that myelin antigen–activated CD4$^+$ T lymphocytes in the 20 MS patients studied express a novel Kv1.3^{high}IKCa1^{low} T_{EM} phenotype.

Repeatedly stimulated control cells acquire the Kv1.3^{high}IKCa1^{low} T_{EM} phenotype. We examined whether myelin-specific control T cells, which belong to the naive and T_{CM} subsets (Figure 2a), could be induced to express the Kv1.3^{high}IKCa1^{low} T_{EM} phenotype by repeated MBP stimulation. Kv1.3, IKCa1, and CCR7 expression was determined 48 hours after the third, seventh, or tenth in vitro stimulation with MBP (Figure 2, b and c). Repeated stimulation caused a progressive decrease of CCR7 and IKCa1 expression and an increase in Kv1.3 levels (Figure 2, b and c). Similar results were obtained with control T cells activated by TT (Figure 2, b and c). Regression analysis revealed a striking inverse correlation between CCR7 and Kv1.3 expression (Pearson correlation coefficient, –0.87, $P < 0.0001$) and a direct correlation between CCR7 and IKCa1 expression (Pearson correlation coefficient, 0.85, P = 0.0004). Since control T cells acquired the Kv1.3^{high}IKCa1^{low} T_{EM} phenotype only after seven to ten antigenic stimulations, the expression of the identical phenotype in short-term myelin-reactive patient cells is most likely the result of repeated in vivo priming by myelin antigens during disease. Repeated activation in vivo by the food antigen ovalbumin might also account for the small percentage (11%) of ovalbumin-activated patient T cells with the Kv1.3^{high} pattern (Figure 1c).

Single-cell confirmation that the Kv1.3^{high}IKCa1^{low} channel pattern is a functional marker for CD4$^+$ activated T_{EM} cells. We confirmed the Kv1.3^{high}IKCa1^{low} channel pattern in antigen-activated T_{EM} cells at the single-cell level by staining for CCR7 and CD45RA and patch clamping immunostained naive, T_{CM}, and T_{EM} cells visualized by fluorescence microscopy (Figure 3a). Activated naive T cells from the peripheral blood of controls were analyzed 48 hours after stimulation with anti-CD3 mAb. Myelin antigen– and TT-activated T_{CM} and T_{EM} cells from the same TCLs were patch clamped 48 hours after the tenth antigenic stimulation.

Fluorescent images of immunostained and patch-clamped CD4$^+$ naive, T_{CM}, and T_{EM} cells are shown in Figure 3a. Naive T cells appeared yellow and T_{CM} cells were green following immunostaining for CCR7 (FITC) and CD45RA (PE). T_{EM} cells stained with PE-

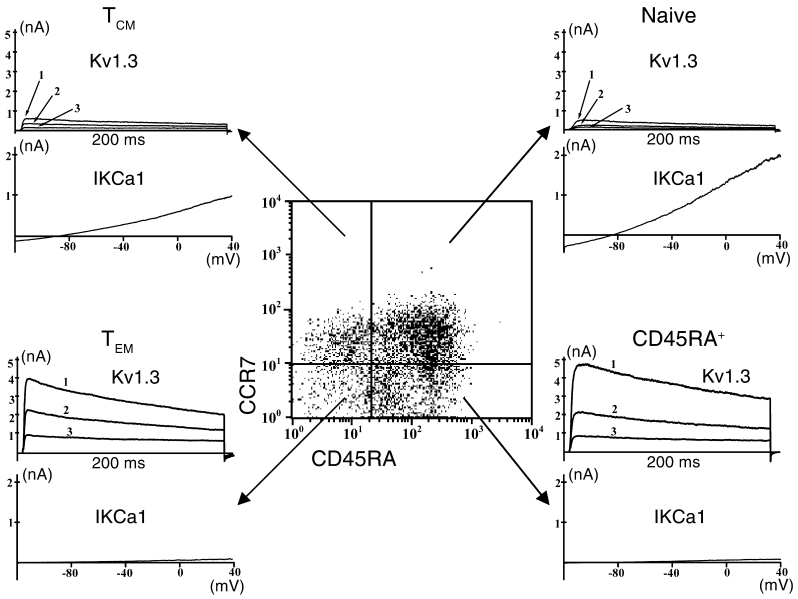

Figure 4
The Kv1.3^{high}IKCa1^{low} phenotype is also found in activated CD8$^+$ effector memory T cells. Flow cytometry profile showing CD45RA and CCR7 expression in activated CD8$^+$ T cells. Representative Kv1.3 and IKCa1 currents from the naive (top right), T_{CM} (top left), T_{EM} (bottom left), and CD45RA$^+$ (bottom right, CCR7$^-$CD45RA$^+$) subsets are shown next to the FACS quadrants.

conjugated anti-CD4 and FITC-tagged anti-CCR7 and anti-CD45RA mAb's exhibited orange fluorescence. Immunostaining did not affect patch-clamp seal formation, membrane capacitance, series resistance, or the biophysical properties of Kv1.3 and IKCa1 currents (data not shown). Substantially larger Kv1.3 currents were observed in activated T_{EM} cells than in activated naive or T_{CM} cells (Figure 3a, bottom panels). Correspondingly, T_{EM} cells activated by MBP or TT expressed more Kv1.3 channels/cell (1,508 ± 97, n = 48 cells) than did MBP- or TT-activated T_{CM} (285 ± 23, n = 25 cells, $P < 0.0001$) or mitogen-activated naive T cells (302 ± 26, n = 14 cells, $P < 0.0001$) (Figure 3b).

Figure 3c summarizes functional expression of Kv1.3 and IKCa1 in the three CD4$^+$ T cell subsets in the resting and activated states. Resting CD4$^+$ T cells (membrane capacitance below 2 pF) of all three subsets exhibited roughly 200–400 Kv1.3 and 0–30 IKCa1 channels. Activation had diametrically opposite consequences for channel expression in the three T cell subsets (Figure 3c). Naive and T_{CM} cells rapidly augmented functional IKCa1 expression following activation (see Figure 6d); this IKCa1 upregulation is most likely transcriptional, as has been reported in normal unseparated peripheral blood T cells and occurs as early as 3 hours after T cell receptor triggering (15). In contrast, activation of T_{EM} cells enhanced Kv1.3 expression without any change in IKCa1 levels. This upregulation is likely to be mediated via the PKC- and calcium-dependent signaling pathways, as we have recently demonstrated in chronically activated encephalitogenic myelin-reactive rat memory cells (19).

CD8$^+$ effector memory cells express the Kv1.3^{high}-IKCa1^{low} channel phenotype. To determine whether the Kv1.3^{high}IKCa1^{low} pattern is a generalized marker for activated T_{EM} cells or whether it is unique to the CD4$^+$ population, we examined Kv1.3 and IKCa1 expression in resting and activated CD8$^+$ T cells. Peripheral blood CD8$^+$ T cells from controls were activated for 48 hours with anti-CD3 mAb, immunostained for CCR7 and CD45RA, and evaluated by FACS and by patch clamping. In the FACS profile shown in Figure 4, four populations are seen on the basis of CCR7 and CD45RA expression: naive, T_{CM}, T_{EM}, and a fourth CCR7$^-$CD45RA$^+$ population. Typical Kv1.3 and IKCa1 traces are shown next to the FACS quadrants of the respective populations. The amplitude of the Kv1.3 currents in activated CD8$^+$ T_{EM} and CCR7$^-$CD45RA$^+$ cells was substantially higher than in activated naive and T_{CM} cells, whereas IKCa1 currents in activated T_{EM} cells were smaller than in activated naive and T_{CM} cells.

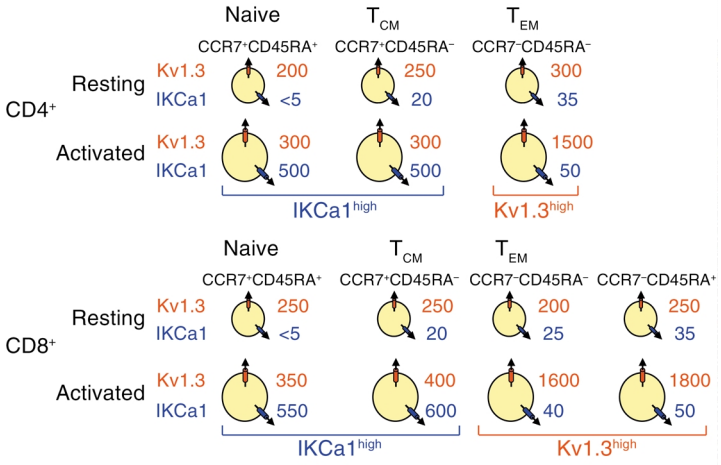

Figure 5
Diagram of average Kv1.3 and IKCa1 channel numbers per cell in the three CD4$^+$ and four CD8$^+$ CCR7/CD45RA-distinguished T cell subsets in the quiescent and the activated state. Mean channel numbers (n = 10–50 cells for each subset) are shown.

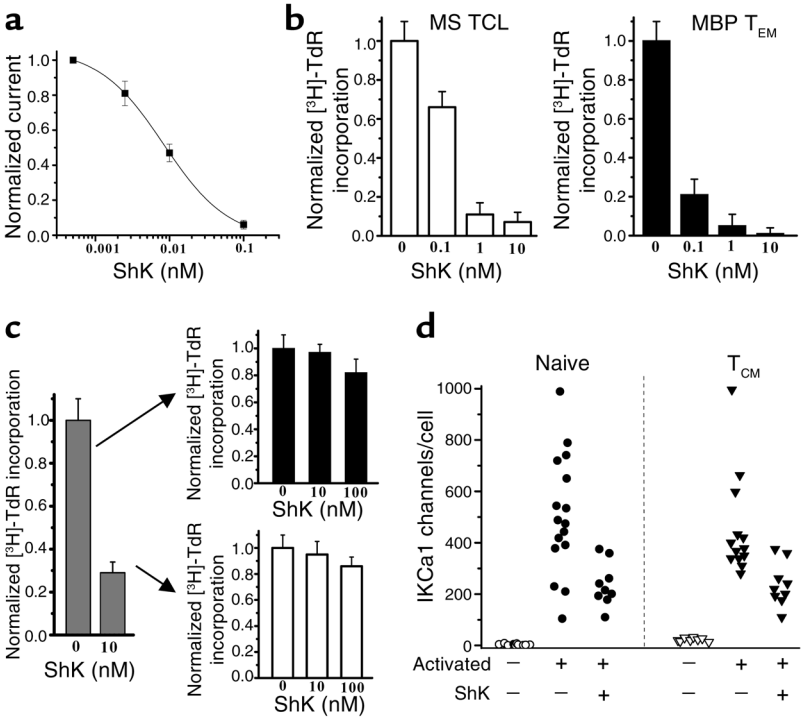

Figure 6
Kv1.3 blockers selectively and persistently suppress MBP-specific T_{EM} cells. (**a**) ShK potently blocked Kv1.3 in Kv1.3^{high}IKCa1^{low} MBP-specific T_{EM} cells K_d, 9 ± 1 pM). Each data point represents the mean ± SD of three cells. (**b**) ShK suppressed anti-CD3 mAb–stimulated [^{3}H]TdR incorporation by a Kv1.3^{high}IKCa1^{low} MBP-specific MS patient TCL stimulated three times with MBP (left) and a control TCL stimulated 12 times with MBP (right). (**c**) ShK (10 nM) partially suppressed anti-CD3 mAb–stimulated [^{3}H]TdR incorporation by normal peripheral blood T lymphocytes (left) but was unable to suppress proliferation when these cells were rechallenged with anti-CD3 mAb. One representative experiment from a total of three experiments is shown. Each experiment was done in triplicate. (**d**) IKCa1 expression is enhanced in activated naive and T_{CM} cells following anti-CD3 mAb stimulation, despite the presence of a suppressive dose of ShK. Open circles, naive resting; filled circles, naive T cells activated by anti-CD3 mAb in the absence or presence of ShK; open triangles, T_{CM} resting; filled triangles, T_{CM} cells activated by anti-CD3 mAb in the absence or presence of ShK.

The diagram in Figure 5 summarizes mean channel numbers in naive and memory subsets in CD4$^+$ and CD8$^+$ lymphocytes before and after activation. Resting (unstimulated) cells of all subsets express about 200–400 Kv1.3 channels per cell along with very few IKCa1 channels. Following activation, CD4$^+$ and CD8$^+$ naive and T_{CM} cells upregulate IKCa1 (500–600 IKCa1 channels expressed per cell), while T_{EM} and CCR7$^-$CD45RA$^+$ cells upregulate Kv1.3 (1,500–1,800 Kv1.3 channels expressed per cell). These results clearly demonstrate that the Kv1.3^{high}IKCa1^{low} channel phenotype is a specific functional marker for activated T_{EM} cell subsets belonging to both the CD4$^+$ and CD8$^+$ populations.

ShK, a potent inhibitor of Kv1.3, persistently suppresses the proliferation of T_{EM} cells. The availability of highly specific Kv1.3 inhibitors (16–18, 30, 34) and the subset-specific expression of the Kv1.3^{high}IKCa1^{low} phenotype raise the possibility of selectively suppressing activated T_{EM} cells without affecting naive or T_{CM} cells. We tested this idea with ShK, a 35-AA polypeptide from the sea anemone *Stichodactyla helianthus,* the most potent known inhibitor of Kv1.3 (16, 30). ShK blocked Kv1.3 channels in CD4$^+$ MBP-specific MS patient T_{EM} TCLs with a K_d of 9 ± 1 pM (Figure 6a). Paralleling the effect on the channel, ShK suppressed anti-CD3 mAb–triggered [^{3}H]TdR incorporation by an MS patient T_{EM} TCL that was stimulated three times with MBP, and a control T_{EM} TCL stimulated 12 times with MBP, with IC_{50} values of 400 pM and 100 pM, respectively (Figure 6b). In contrast, ShK was tenfold less effective (IC_{50}, 4 nM) in suppressing anti-CD3 mAb–stimulated [^{3}H]TdR incorporation by control peripheral blood lymphocytes consisting mainly of naive and T_{CM} cells (Figure 6c), possibly because these cells rapidly upregulate IKCa1 after stimulation and become less sensitive to Kv1.3 inhibitors (15). Consistent with this interpretation, peripheral blood T cells activated for 48 hours (to upregulate IKCa1), rested for 12 hours, and then rechallenged with anti-CD3 mAb for a further 48 hours were completely insensitive to ShK (upper arrow in Figure 6c). Surprisingly, cells that had been suppressed by ShK in the first round of stimulation, when rested and rechallenged with anti-CD3 mAb, were also resistant to ShK (lower arrow in Figure 6c). A plausible explanation for this result is that ShK, at concentrations that suppress proliferation, cannot prevent the upregulation of IKCa1 during the activation process.

To test this idea, we examined the effect of ShK on anti-CD3 mAb–induced upregulation of IKCa1 expression in naive and T_{CM} peripheral blood T cells. IKCa1 channels were virtually undetectable in resting naive cells, and resting T_{CM} cells expressed 20 ± 3 IKCa1 channels/cell (Figure 6d). Activation produced a dramatic augmentation of IKCa1 expression in both subsets, the mean channel number/cell being 520 ± 76 (n = 16 cells) and 451 ± 54 (n = 13 cells) in activated naive and T_{CM} cells, respectively (Figure 6d). Kv1.3 expression did not change in either subset (data not shown). Despite not proliferating (Figure 6c), naive and T_{CM} cells exposed to ShK also increased IKCa1 expression (naive, 237 ± 28 channels/cell, n = 9 cells; T_{CM}, 230 ± 47 channels/cell, n = 9 cells) (Figure 6d). Although the IKCa1 levels in ShK-treated cells were lower than in activated cells (naive, P = 0.003; T_{CM}, P = 0.006), the channel number was sufficient to promote T cell activation, as evidenced by the normal proliferative response to a second stimulus and by the insensitivity to Kv1.3 blockade (Figure 6c, lower arrow). These results indicate that Kv1.3 inhibitors persistently shut down the function of T_{EM} cells, while naive and T_{CM} cells are initially less sensitive to Kv1.3 blockade and then escape inhibition by upregulating IKCa1.

Discussion

Using whole-cell patch-clamp recording, we identified a distinctive Kv1.3^{high}IKCa1^{low} K^+ channel expression pattern in activated human T_{EM} cells. Unlike naive and T_{CM} cells that upregulate IKCa1 with little change in Kv1.3 expression during activation (15, 16) (Figure 1 and Figure 4), T_{EM} cells enhanced Kv1.3 levels with a minimal increase in IKCa1 (Figure 1). The subset-specific channel expression in T_{EM} cells allowed us to selectively suppress the proliferation of T_{EM} cells with a high-affinity Kv1.3 blocker. Activated myelin-specific T cells from MS patients exhibited the Kv1.3^{high}IKCa1^{low} T_{EM} phenotype, corroborating earlier reports that these cells exhibit features of chronically stimulated memory T cells (1–4). In contrast, patient T cells activated with other antigens (GAD65, insulin peptide, or ovalbumin) or with mitogens did not exhibit this phenotype. The myelin-reactive Kv1.3^{high}IKCa1^{low} T_{EM} cells may arise as a consequence of repeated activation by myelin antigens during the disease process and potentially contribute to MS pathogenesis due to their propensity to home to inflamed tissues and secrete copious amounts of inflammatory cytokines such as IFN-γ and TNF-α (24, 25). In support of this idea, adoptive transfer of Kv1.3^{high}IKCa1^{low} memory T cells produces severe EAE in rats, the Kv1.3 levels in these cells correlating with their encephalitogenicity (18, 23, 35).

The Kv1.3^{high}IKCa1^{low} pattern is found in activated $CD4^+$ and $CD8^+$ T_{EM} cells, suggesting that it is a functionally relevant marker for both these subsets. At rest, T_{EM} cells express 200–400 Kv1.3 channels with few or no IKCa1 channels, similar to naive and T_{CM} cells (Figure 3c and Figure 5). However, activation has significantly different consequences in the three T cell subsets. Activation of naive and T_{CM} cells results in rapid augmentation of functional IKCa1 expression (Figure 6d); this IKCa1 upregulation is most likely transcriptional, as has been reported in normal unseparated peripheral blood T cells, and occurs as early as 3 hours after T cell receptor triggering (15). In contrast, activation of T_{EM} cells enhances Kv1.3 expression without any change in IKCa1 levels. The differential expression of the two types of K^+ channels can not only be used as a marker for T_{EM} cells but could also be exploited in a therapeutic strategy that selectively suppresses the proliferation of activated T_{EM} cells with Kv1.3-specific blockers.

ShK, a potent Kv1.3 inhibitor, suppressed proliferation of T_{EM} cells tenfold more effectively than it suppressed proliferation of peripheral blood T cells comprised primarily of naive and T_{CM} cells, because the latter cells, although initially dependent on Kv1.3 channels, escaped Kv1.3 inhibition by rapidly upregulating IKCa1. Upon reactivation, naive and T_{CM} cells with upregulated IKCa1 were resistant to further Kv1.3 blockade (Figure 6c), consistent with previous reports that preactivated peripheral blood T cells are resistant to Kv1.3 inhibitors and sensitive to IKCa1 inhibitors when reactivated (15). Thus, IKCa1 rapidly becomes the functionally dominant K^+ channel in naive and T_{CM} cells during the activation process. In contrast, T_{EM} cells never upregulate IKCa1, and Kv1.3 blockers therefore produce persistent suppression of this T cell subset. These results suggest radically different functional requirements for Kv1.3 and IKCa1 in the three subsets.

Differences in the ratio of IKCa1 and Kv1.3 channel numbers have been reported to contribute to the variability in the amplitude and shape of the Ca^{2+} signal in lymphocytes. Ca^{2+} may rise transiently or exhibit oscillations or increase in a sustained fashion (36). Both K^+ channels provide the counterbalancing cation efflux that maintains calcium influx over the time scale required for gene transcription mediated by nuclear factor of activated T cells (NFAT) and for IL-2 production during T cell activation (37, 38). In lymphocytes where IKCa1 predominates (e.g., activated naive and T_{CM} cells), calcium entry is tightly coupled to the opening of IKCa1 channels, which results in membrane hyperpolarization and an increased tendency to exhibit an oscillatory Ca^{2+} signal in response to T cell receptor triggering (36, 39–41). Differences in the Ca^{2+} signaling pattern in cells dominated by Kv1.3 (T_{EM} cells) versus IKCa1 (naive and T_{CM} cells) might have important functional consequences, because the functional readout of cells in response to antigenic stimulation is modulated by the shape and nature of the Ca^{2+} signal (42, 43). Kv1.3 might also promote trafficking of T_{EM} cells to inflamed tissues via its reported role in cell adhesion and migration (44, 45).

Since the majority of myelin-specific MS patient T cells are Kv1.3^{high}IKCa1^{low} T_{EM} cells and their proliferation is potently blocked by ShK, a Kv1.3-based therapeutic strategy that specifically targets T_{EM} cells may

ameliorate symptoms of MS without significant impairment of the immune response. In support of this therapeutic approach, Kv1.3 blockers prevented lethal adoptive EAE in rats caused by Kv1.3^{high}IKCa1^{low} myelin-specific memory rat T cells, and administration of Kv1.3 inhibitors after the onset of symptoms significantly ameliorated disease (18, 23). No obvious side effects from Kv1.3 blockers were observed in this trial, possibly due to the channel's restricted tissue distribution (16–18, 29, 30, 34).

Although Kv1.3 blockers would suppress all activated T_{EM} cells, especially cells specific for chronic infectious agents or for vaccine antigens, and potentially be less selective than antigen-specific strategies, they would still have a significant advantage over generalized immunomodulators currently used for therapy. Furthermore, under conditions where epitope spreading (46) occurs (i.e., the expansion and activation of T cells against a multiplicity of myelin antigens during the progression of MS), antigen-specific vaccination strategies may be difficult, and the less selective approach of targeting T_{EM} cells with Kv1.3 blockers might have significant therapeutic value.

An extensive effort by the pharmaceutical industry has yielded several small molecules that inhibit Kv1.3 at nanomolar concentrations, including correolide, sulfimidebenzamidoindanes, phenyloxoazapropylcycloalkanes, and dihydropyrimidines (17, 47, 48). These are in various stages of development as immunosuppressants. In conclusion, selective Kv1.3 blockers may represent a new therapy for MS and other T cell–mediated autoimmune diseases (e.g., type 1 diabetes mellitus) in which autoreactive memory cells contribute to pathogenesis (5). The excellent track record of K^+ channel blockers in the management of epilepsy, stroke, and cardiac arrhythmias enhances the attractiveness of this therapeutic approach.

Acknowledgments

This work was supported by grants from the National Multiple Sclerosis Society (to K.G. Chandy and P.A. Calabresi), NIH (MH-59222 to K.G. Chandy and NS-41435 to P.A. Calabresi), the Rockefeller Brothers Fund (to K.G. Chandy), and by postdoctoral fellowships from the National Multiple Sclerosis Foundation (C. Beeton) and the American Heart Association (H. Wulff). The authors are deeply indebted to George A. Gutman, Michael D. Cahalan, Jay Gargus, James Hall, and Harry Haigler for critically reading the manuscript and for their helpful suggestions.

1. Allegretta, M., Nicklas, J.A., Sriram, S., and Albertini, R.J. 1990. T cells responsive to myelin basic protein in patients with multiple sclerosis. *Science.* **247**:718–721.
2. Lovett-Racke, A.E., et al. 1998. Decreased dependence of myelin basic protein-reactive T cells on CD28-mediated costimulation in multiple sclerosis patients: a marker of activated/memory T cells. *J. Clin. Invest.* **101**:725–730.
3. Scholz, C., Anderson, D.E., Freeman, G.J., and Hafler, D.A. 1998. Expansion of autoreactive T cells in multiple sclerosis is independent of exogenous B7 costimulation. *J. Immunol.* **160**:1532–1538.
4. Markovic-Plese, S., Cortese, I., Wandinger, K.P., McFarland, H.F., and Martin, R. 2001. CD4$^+$CD28$^-$ costimulation-independent T cells in multiple sclerosis. *J. Clin. Invest.* **108**:1185–1194. doi:10.1172/JCI200112516.
5. Viglietta, V., Kent, S.C., Orban, T., and Hafler, D.A. 2002. GAD65-reactive T cells are activated in patients with autoimmune type 1a diabetes. *J. Clin. Invest.* **109**:895–903. doi:10.1172/JCI200214114.
6. Friedrich, M., et al. 2000. Flow cytometric characterization of lesional T cells in psoriasis: intracellular cytokine and surface antigen expression indicates an activated, memory effector/type 1 immunophenotype. *Arch. Dermatol. Res.* **292**:519–521.
7. Hohlfeld, R., and Wekerle, H. 2001. Immunological update on multiple sclerosis. *Curr. Opin. Neurol.* **14**:299–304.
8. Steinman, L. 2001. Multiple sclerosis: a two-stage disease. *Nat. Immunol.* **2**:762–764.
9. O'Connor, K., Bar-Or, A., and Hafler, D.A. 2001. The neuroimmunology of multiple sclerosis: possible roles of T and B lymphocytes in immunopathogenesis. *J. Clin. Immunol.* **21**:81–92.
10. Holoshitz, J., Naparstek, Y., Ben-Nun, A., Marquardt, P., and Cohen, I.R. 1984. T lymphocyte lines induce autoimmune encephalomyelitis, delayed hypersensitivity and bystander encephalitis or arthritis. *Eur. J. Immunol.* **14**:729–734.
11. 't Hart, B.A., et al. 2000. A new primate model for multiple sclerosis in the common marmoset. *Immunol. Today.* **21**:290–297.
12. DeCoursey, T.E., Chandy, K.G., Gupta, S., and Cahalan, M.D. 1984. Voltage-gated K^+ channels in human T lymphocytes: a role in mitogenesis? *Nature.* **307**:465–468.
13. Chandy, K.G., DeCoursey, T.E., Cahalan, M.D., McLaughlin, C., and Gupta, S. 1984. Voltage-gated potassium channels are required for human T lymphocyte activation. *J. Exp. Med.* **160**:369–385.
14. Lewis, R.S., and Cahalan, M.D. 1995. Potassium and calcium channels in lymphocytes. *Annu. Rev. Immunol.* **13**:623–653.
15. Ghanshani, S., et al. 2000. Up-regulation of the IKCa1 potassium channel during T-cell activation: molecular mechanism and functional consequences. *J. Biol. Chem.* **275**:37137–37149.
16. Cahalan, M.D., Wulff, H., and Chandy, K.G. 2001. Molecular properties and physiological roles of ion channels in the immune system. *J. Clin. Immunol.* **21**:235–252.
17. Chandy, K.G., et al. 2001. Potassium channels in T lymphocytes: toxins to therapeutic immunosuppressants. *Toxicon.* **39**:1269–1276.
18. Beeton, C., et al. 2001. Selective blockade of T lymphocyte K+ channels ameliorates experimental autoimmune encephalomyelitis, a model for multiple sclerosis. *Proc. Natl. Acad. Sci. U. S. A.* **98**:13942–13947.
19. Beeton, C., et al. 2003. A novel fluorescent toxin to detect and investigate Kv1.3-channel up-regulation in chronically activated T lymphocytes. *J. Biol. Chem.* **278**:9928–9937.
20. Matteson, D.R., and Deutsch, C. 1984. K channels in T lymphocytes: a patch clamp study using monoclonal antibody adhesion. *Nature.* **307**:468–471.
21. Cahalan, M.D., Chandy, K.G., DeCoursey, T.E., and Gupta, S. 1985. A voltage-gated potassium channel in human T lymphocytes. *J. Physiol.* **358**:197–237.
22. Deutsch, C., Krause, D., and Lee, S.C. 1986. Voltage-gated potassium conductance in human T lymphocytes stimulated with phorbol ester. *J. Physiol.* **372**:405–423.
23. Beeton, C., et al. 2001. Selective blocking of voltage-gated K^+ channels improves experimental autoimmune encephalomyelitis and inhibits T cell activation. *J. Immunol.* **166**:936–944.
24. Sallusto, F., Lenig, D., Forster, R., Lipp, M., and Lanzavecchia, A. 1999. Two subsets of memory T lymphocytes with distinct homing potentials and effector functions. *Nature.* **401**:708–712.
25. Geginat, J., Sallusto, F., and Lanzavecchia, A. 2001. Cytokine-driven proliferation and differentiation of human naive, central memory, and effector memory CD4$^+$ T cells. *J. Exp. Med.* **194**:1711–1719.
26. Hemmer, B., et al. 1996. Cytokine phenotype of human autoreactive T cell clones specific for the immunodominant myelin basic protein peptide 83-99. *J. Neurosci. Res.* **45**:852–862.
27. Calabresi, P.A., Martin, R., and Jacobson, S. 1999. Chemokines in chronic progressive neurological diseases: HTLV-1 associated myelopathy and multiple sclerosis. *J. Neurovirol.* **5**:102–108.
28. Martin, R., Voskuhl, R., Flerlage, M., McFarlin, D.E., and McFarland, H.F. 1993. Myelin basic protein-specific T-cell responses in identical twins discordant or concordant for multiple sclerosis. *Ann. Neurol.* **34**:524–535.
29. Grissmer, S., et al. 1990. Expression and chromosomal localization of a lymphocyte K+ channel gene. *Proc. Natl. Acad. Sci. U. S. A.* **87**:9411–9415.
30. Kalman, K., et al. 1998. ShK-Dap^{22}, a potent Kv1.3-specific immunosuppressive polypeptide. *J. Biol. Chem.* **273**:32697–32707.
31. Wulff, H., et al. 2000. Design of a potent and selective inhibitor of the intermediate-conductance Ca^{2+}-activated K^+ channel, IKCa1: a potential immunosuppressant. *Proc. Natl. Acad. Sci. U. S. A.* **97**:8151–8156.
32. Atkinson, M.A., and Maclaren, N.K. 1994. The pathogenesis of insulin-dependent diabetes mellitus. *N. Engl. J. Med.* **331**:1428–1436.

33. Alleva, D.G., et al. 2001. A disease-associated cellular immune response in type 1 diabetics to an immunodominant epitope of insulin. *J. Clin. Invest.* **107**:173–180.
34. Koo, G.C., et al. 1997. Blockade of the voltage-gated potassium channel Kv1.3 inhibits immune responses in vivo. *J. Immunol.* **158**:5120–5128.
35. Strauss, U., Schubert, R., Jung, S., and Mix, E. 1998. K^+ currents of encephalitogenic memory T cells decrease with encephalitogenicity while interleukin-2 (IL-2) receptor expression remains stable during IL-2 dependent expansion. *Receptors Channels.* **6**:73–87.
36. Verheugen, J.A., and Vijverberg, H.P. 1995. Intracellular Ca^{2+} oscillations and membrane potential fluctuations in intact human T lymphocytes: role of K^+ channels in Ca^{2+} signaling. *Cell Calcium.* **17**:287–300.
37. Clipstone, N.A., and Crabtree, G.R. 1992. Identification of calcineurin as a key signalling enzyme in T-lymphocyte activation. *Nature.* **357**:695–697.
38. Timmerman, L.A., Clipstone, N.A., Ho, S.N., Northrop, J.P., and Crabtree, G.R. 1996. Rapid shuttling of NF-AT in discrimination of Ca^{2+} signals and immunosuppression. *Nature.* **383**:837–840.
39. Grissmer, S., Nguyen, A.N., and Cahalan, M.D. 1993. Calcium-activated potassium channels in resting and activated human T lymphocytes. Expression levels, calcium dependence, ion selectivity, and pharmacology. *J. Gen. Physiol.* **102**:601–630.
40. Hess, S.D., Oortgiesen, M., and Cahalan, M.D. 1993. Calcium oscillations in human T and natural killer cells depend upon membrane potential and calcium influx. *J. Immunol.* **150**:2620–2633.
41. Fanger, C.M., et al. 2001. Calcium-activated potassium channels sustain calcium signaling in T lymphocytes. *J. Biol. Chem.* **276**:12249–12256.
42. Dolmetsch, R.E., Xu, K., and Lewis, R.S. 1998. Calcium oscillations increase the efficiency and specificity of gene expression. *Nature.* **392**:933–936.
43. Lewis, R.S. 2001. Calcium signaling mechanisms in T lymphocytes. *Ann. Rev. Immunol.* **19**:497–521.
44. Levite, M., et al. 2000. Extracellular K^+ and opening of voltage-gated potassium channels activate T cell integrin function: physical and functional association between Kv1.3 channels and beta1 integrins. *J. Exp. Med.* **191**:1167–1176.
45. Artym, V.V., and Petty, H.R. 2002. Molecular proximity of the Kv1.3 voltage-gated potassium channel and beta1-integrins on the plasma membrane of melanoma cells: effects of cell adherence and channel blockers. *J. Gen. Physiol.* **120**:29–37.
46. Vanderlugt, C.L., and Miller, S.D. 2002. Epitope spreading in immune-mediated diseases: implications for immunotherapy. *Nat. Rev.* **2**:85–95.
47. Koo, G.C., et al. 1999. Correolide and derivatives are novel immunosuppressants blocking the lymphocyte Kv1.3 potassium channels. *Cell. Immunol.* **197**:99–107.
48. Schmalhofer, W.A., et al. 2002. Identification of a new class of inhibitors of the voltage-gated potassium channel, Kv1.3, with immunosuppressant properties. *Biochemistry.* **18**:7781–7794.